(18) Hashimoto, T.; Fujimura, M.; Kawai, H. *Macromolecules* **1980**, *13*, 1660.
(19) Annighofer, F.; Gronski, W. *Makromol. Chem.* **1984**, *185*, 2213.
(20) Richards, R. W.; Thomason, J. L. *Polymer* **1983**, *24*, 1089.
(21) Richards, R. W.; Thomason, J. L. *Polymer* **1983**, *24*, 275.
(22) Richards, R. W.; Thomason, J. L. *Polymer* **1981**, *22*, 581.
(23) Hadziioannou, G.; Picot, C.; Skoulios, A.; Ionescu, M.; Mathis, A.; Duplessix, R.; Gallot, Y.; Lingelser, J. *Macromolecules* **1982**, *15*, 263.
(24) Richards, R. W.; Thomason, J. L. *Macromolecules* **1983**, *16*, 982.
(25) Bates, F. S.; Dierker, S. B.; Wignall, G. D. *Macromolecules* **1986**, *19*, 1938.
(26) Leung, L. M.; Koberstein, J. T. *Macromolecules* **1986**, *19*, 706.
(27) Hashimoto, T.; Tsukahara, Y.; Tachi, K.; Kawai, H. *Macromolecules* **1983**, *16*, 648.
(28) Kraus, G.; Rollmann, K. W. *J. Polym. Sci., Polym. Phys. Ed.* **1976**, *14*, 1133.
(29) Diamant, J.; Soong, D. S.; Williams, M. C. In *Contemporary Topics in Polymer Science*; Bailey, W. J., Tsurata, T., Eds.; Plenum: New York, 1984; Vol. 4.
(30) Annighofer, F.; Gronski, W. *Colloid Polym. Sci.* **1983**, *261*, 15.
(31) Gronski, W.; Annighofer, F.; Stadler, R. *Makromol. Chem. Suppl.* **1984**, *6*, 141.
(32) Henderson, C. P.; Williams, M. C. *Polymer* **1985**, *26*, 2021.
(33) Wu, S.; Chuang, H.; Han, C. D. *J. Polym. Sci., Polym. Phys. Ed.* **1986**, *24*, 143.
(34) Henderson, C. P.; Williams, M. C. *Polymer* **1985**, *26*, 2026.
(35) Reimer, L. *Transmission Electron Microscopy: Physics of Image Formation and Microanalysis*; Springer-Verlag: New York, 1984; pp 108–109, 185–205.
(36) Spontak, R. J. In *Proceedings of the 44th Annual Meeting of the Electron Microscopy Society of America*; Bailey, G. W., Ed.; San Francisco Press: San Francisco, 1986; p 788.
(37) Spontak, R. J.; Williams, M. C.; Agard, D. A. *Polymer*, in press.
(38) Spontak, R. J.; Williams, M. C.; Schooley, C. N. *J. Mater. Sci.* **1986**, *21*, 3173.
(39) Thomas, H. R.; O'Malley, J. J. *Macromolecules* **1979**, *12*, 323.
(40) O'Malley, J. J.; Thomas, H. R.; Lee, G. M. *Macromolecules* **1979**, *12*, 996.
(41) Russ, J. C.; Russ, J. Ch. In *Microbeam Analysis 1986*; Romig, A. D., Ed.; San Francisco Press: San Francisco, 1986; p 501.
(42) Grum, F.; Becherer, R. J. *Optical Radiation Measurements: Radiometry*; Academic: New York, 1979; p 21–23.
(43) Zielinski, J. M. M.S. Thesis, University of California, Berkeley, 1986.
(44) Meier, D. J. In *Proceedings, Polymer Colloqium*; Kyoto, Japan, Sept 1977.
(45) Stadler, R.; Gronski, W. *Colloid Polym. Sci.* **1982**, *262*, 466.
(46) Hadziioannou, G.; Skoulios, A. *Macromolecules* **1982**, *15*, 258.
(47) Douy, A.; Gallot, B. *Makromol. Chem.* **1972**, *156*, 81.
(48) Pedemonte, E.; Alfonso, G. C. *Macromolecules* **1975**, *8*, 85.
(49) Krigbaum, W. R.; Yazgan, S.; Tolbert, W. R. *J. Polym. Sci., Polym. Phys. Ed.* **1973**, *11*, 511.
(50) Mills, P. J.; Green, P. F.; Palmstrom, C. J.; Mayer, J. W.; Kramer, E. J. *J. Polym. Sci., Polym. Phys. Ed.* **1986**, *24*, 1.
(51) Spontak, R. J., unpublished calculations for Ph.D. in progress, University of California, Berkeley, 1986.

Cylindrical Micelles Formed by a Charged Comb-Shaped Copolymer in Aqueous Solutions Studied by Small-Angle Neutron Scattering

L. B. Shih,*[†] E. Y. Sheu,[‡] and S. H. Chen[§]

Polymer Research Department, S. C. Johnson & Son, Inc., Racine, Wisconsin 53403, and Department of Nuclear Engineering, Massachusetts Institute of Technology, Cambridge, Massachusetts 02139. *Received July 6, 1987; Revised Manuscript Received October 23, 1987*

ABSTRACT: We present the analysis of a series of small-angle neutron scattering data of a comb-shaped copolymer, poly(1-octadecene-*co*-(maleic anhydride)), dissolved at various concentrations in D_2O at room temperature. The results show at full ionization the copolymers self-associate to form cylindrical micelles with a radius of 27 Å and a length of 99 Å. At low concentrations, the number of repeating units of the copolymer per micelle is determined to be 233 ± 5 and the hydration number per hydrophilic head group equals 10. The number of repeating units gradually decreases to 98 with concomitant increase in the hydration number to 30 at 20 wt % solution. This indicates that the system tends to lower its free energy by decreasing the aggregation number of micelles at higher concentrations.

I. Introduction

Synthetic polyelectrolytes in aqueous solutions have been the focus of many studies.[1-3] These polymers are important in many industrial applications because the conformational states of these polymers in solution often influence the solution behavior, such as the rheological property. Especially interesting are some polyelectrolytes with amphiphilic characteristics; they exhibit waxy properties and yet are soluble in water.

Our main interest in this work is the aggregational behavior of a comb-shaped alternating copolymer poly(1-octadecene-*co*-(maleic anhydride)), abbreviated as PODMA, in water. The copolymers form clear solutions at moderate concentrations when the diacid groups are fully neutralized with the hydroxides of alkaline metal ions. The molecular structure of one repeating unit in the diacid form is depicted in Figure 1. Earlier studies with a similar class of copolymer, (alkyl vinyl ether)-*co*-(maleic anhydride), by Dubin and Strauss[2-5] using potentiometric titrations and viscosity measurements have shown that the conformational states of these polymers are strongly influenced by the degree of ionization of the diacid head group. Their studies were centered around copolymers with shorter side chains in comparison to PODMA. They proposed that the copolymers form hypercoiled "intramolecular" micelles. However, our recent solubilization measurements of PODMA using Raman and FTIR[6] have clearly shown the partition of benzyl alcohol in the hydrocarbon and aqueous phases. The results are indicative of the formation of hydrocarbon domains in water.

Carbon-13 NMR measurements[7] of PODMA solutions have shown that the chemical shifts of the side-chain methylene groups (C_5–C_{14}) are unchanged in solutions with concentrations ranging from 50 to 2000 ppm. Similar measurements with sodium alkylsulfates and other surfactants[8,9] have demonstrated that the chemical shift

---

[†] S. C. Johnson & Son, Inc.

[‡] Massachusetts Institute of Technology. Present address: Exxon Research & Engineering Co., Clinton Township, Annandale, NJ 08801.

[§] Massachusetts Institute of Technology.

0024-9297/88/2221-1387$01.50/0 © 1988 American Chemical Society

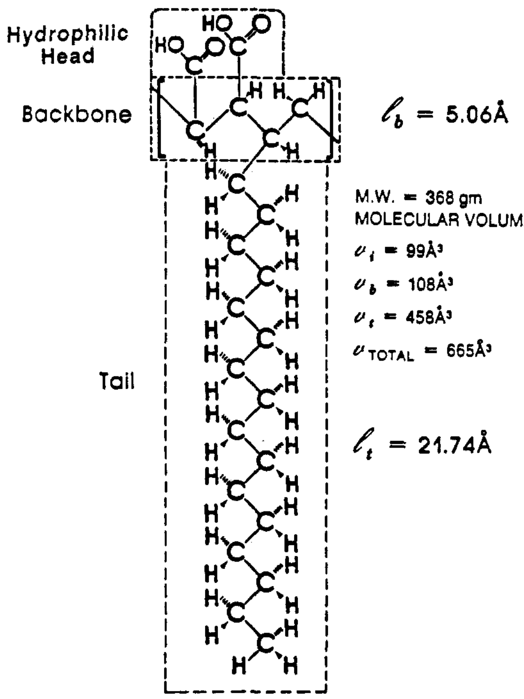

Figure 1. Molecular structure of one repeating unit of poly(1-octadecene-*co*-(maleic anhydride)) in the diacid form.

versus inverse concentration plot shows an inflection point at the critical micelle concentration. We expected to observe the same behavior if the copolymer aggregates were to dissociate into molecular states. The NMR results have clearly demonstrated that even if there is a critical micelle concentration for this copolymer it would be below 50 ppm, which is the practical lower limit for the NMR. However, from the NMR data, it is not conclusive whether the micelles are formed through intermolecular aggregation or intramolecular hypercoils. Differential scanning calorimetry measurements of solutions at a wide range of concentrations have shown no thermal event between the freezing and boiling points of D_2O, indicating that the side chains and the micelles are probably in the same state of conformation at this temperature and concentration range.

In this work, we first used the small angle neutron scattering (SANS) technique to investigate PODMA in water where the interactions between aggregates are weak; hence the analysis of the cross section over the entire Q-range can be made without ambiguity. In this case, the cross section at zero angle limit gives the absolute molecular weight of the aggregates and the cross section at large angles gives the shape of aggregates. Thus the micellar formation and its geometric shape can be unambiguously established. At higher concentrations the interaction between charged aggregates becomes appreciable and the information with regard to the aggregation number and shape of the micelles can only be inferred from an asymptotic analysis of the large-angle data.

In section II, we briefly summarize the experimental procedures. In section III we present the cross-section formula for cylindrical micelles, and in section IV we present data analysis using this formula and the results. The major findings and conclusions are summarized in section V. A preliminary description of this work can be found in a recent Materials Research Society Conference Proceedings.[10]

II. Experimental Section

The alternating addition copolymer can be synthesized via free-radical initiation. Several procedures are in existence in synthesizing this class of copolymers.[11] Typically, an equivalent amount of maleic anhydride is added dropwise to a container containing 1-alkene and a peroxide initiator maintained at 160 °C and under N_2 while stirring. The polymerization is often complete about 30 min after the completion of the addition of maleic anhydride.

The copolymer used in this study was purified by removing the trace amount of the unreacted 1-alkene. The elemental analysis of the copolymer in the anhydride form showed that the mole ratio of maleic anhydride to 1-alkene was 1.2 to 1. The weight-average and number-average molecular weights of PODMA were determined by gel permeation chromatography to be $M_w/M_n = 6660/3960 = 1.68$ by using polystyrene standards. The new set of data was slightly different from our previous report,[10] mainly due to the use of an improved method to remove base-line noise from the chromatogram.[12] The T_g of the copolymer is 330 K and the T_m of the side-chain 258 K.

The solutions for SANS study were prepared by combining hydrogenated copolymer with a stoichiometric quantity of LiOH to fully neutralize the diacid head groups in a given amount of D_2O. The stoichiometry of neutralization was experimentally verified by monitoring the disappearance of the -COOH band with FTIR. The solutions were heated to 95 ± 5 °C for 10–35 hours, depending on the concentrations, until they became clear or translucent. LiOH was from Fisher specified as purified and anhydrous and was used as received. D_2O was from Aldrich specified as 100% D atom.

SANS data for the low concentration series (0.25–1.0% by weight) were taken at the National Center for small-angle scattering research at Oak Ridge National Laboratory. This series of data was taken at the wave length $\lambda = 4.75$ Å. The Bragg wavenumber Q is related to wavelength, λ, and scattering angle, θ, by $Q = (4\pi/\lambda)\sin(\theta/2)$, and covered the range 0.02–0.15 $Å^{-1}$. The high concentration series (10–20%) was taken at the biology low-angle spectrometer in Brookhaven National Laboratory. The wavelength was 5.32 Å and the Q range was 0.015–0.26 $Å^{-1}$. The raw data were corrected for background, the empty cell contributions, and the nonuniform detector efficiencies and then normalized by using a 1 mmH_2O sample. The normalized intensity $I(Q)$ is given in the unit of cm^{-1}. In the following analysis of data, we subtracted the incoherent scattering contributions from the calculated amounts of hydrogen and deuterium atoms in the solution.

III. Cross Section Formula for Cylindrical Micelles

We first assume a system of monodispersed and isotropically oriented cylinders of length L and cross sectional radius A dispersed in D_2O. Although the following formulas are derived under the assumption of monodispersity, it will become clear later that the cylinder length L represents the weight average of the degree of polymerization and that the polydispersity of the cylinders is thus reflected in the SANS data.

The normalized cross section $I(Q)$ can be written as

$$I(Q) = I_0\tilde{P}(Q)\tilde{S}(Q) \tag{1}$$

where $\tilde{P}(Q)$ is the normalized cylindrical form factor given by (13),

$$\tilde{P}(Q) = \int_0^1 d\mu \left[\frac{2J_1(V)}{V}\frac{\sin w}{w}\right]^2 \tag{2}$$

In eq 2, μ is the direction cosine between the Q vector and the axis of the cylinder, $V = QR(1-\mu^2)^{1/2}$, and $w = Q\mu L/2$. $\tilde{S}(Q)$ is an angular-averaged structure factor of interacting cylinders.[14] This factor is unity for all Q in the dilute limit and at sufficiently large Q in the case of high concentrations. At high concentrations, $I(Q)$ is expected to show a peak at a Q value corresponding to 2π divided by the characteristic periodic distance of the local ordering of the cylinders. The I_0 factor can be related to the repeating unit concentration (number of repeating units per unit

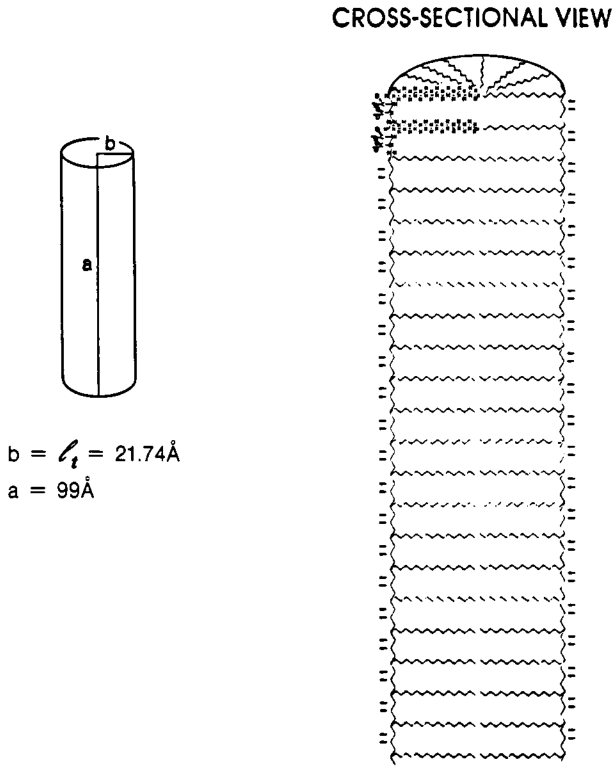

Figure 2. Cylindrical micelle formed by the fully ionized, comb-shaped copolymer poly(1-octadecene-*co*-(maleic anhydride)) in water.

volume), the geometrical factors of the repeating unit and the polymer in the following way:

$$I_0 = c_m PN(b_m - V_m\rho_s)^2 \qquad (3)$$

where c_m is the repeating unit concentration, P is the degree of polymerization (or the weight average of the degree of polymerization in the case of polydispersity), N is the aggregation number of the micelle (number of copolymer molecules per micelle), $b_m = 2.73 \times 10^{-12}$ cm is the scattering length of one repeating unit, $V_m = 665$ Å^3 is the dry volume of one repeating unit, and $\rho_s = 6.34 \times 10^{10}$ cm^{-2} is the scattering length density of the solvent D_2O.

In fitting the SANS data with eq 1 we impose the volume conservation constraint so that the total volume of a micelle is the sum of the dry volume of all the repeating units and the volume of hydrated water molecules. Denoting N_{D_2O} as the number of water molecules associated with the head group of one repeating unit,

$$L\pi R^2 = PN(V_m + 30N_{D_2O}) \qquad (4)$$

Equation 1 together with eq 4 implies that there are three adjustable parameters, namely, R, L, and PN, in the theory in the region where $\bar{S}(Q)$ is unity.

IV. Data Analysis and Results

Figure 2 depicts the packing of the fully ionized copolymers in a cylindrical form where the core of the cylinder is filled up with side chains and the backbone of the copolymer runs along the length of the cylinder. We have found that the data fall into two groups: the low concentration regime and the high concentration regime. Since these two groups of data were taken from two different spectrometers, the absolute intensity calibration was checked with a pair of samples at a common concentration of 10 wt % and the results showed good agreement. The normalized intensity divided by the repeating unit concentration for the dilute series is plotted in Figure 3a and that for concentrated series in Figure 3b. It should be noted that at the lowest concentration (0.25%) there is no interaction peak. But as the concentration goes up, the interaction peak gradually builds up at around $Q_{max} = 0.05$ Å^{-1} which corresponds to a periodic distance of 126 Å. We fit the low concentration series data to eq 1 by setting $\bar{S}(Q)$ equal to 1 for Q range 0.0266–0.15 Å^{-1}. The results of the fit are shown in Figure 4, which demonstrates good agreement between the fitted curves (solid lines) and the experimental data for all Q. The χ values for all cases are between 0.9 and 1.2. The extracted parameters are found to be uniquely determined in this analysis. The parame-

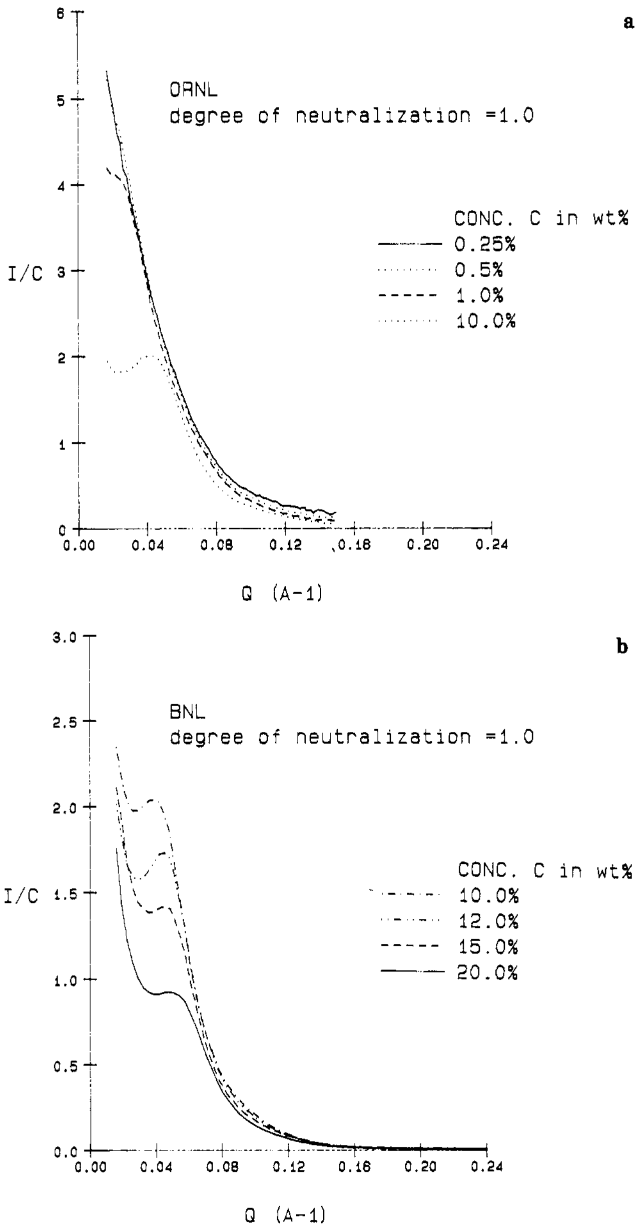

Figure 3. Normalized intensity distribution divided by the repeating unit concentration, c_m, for dilute regime (a, top) and concentrated regime (b, bottom).

Table I
Summary of Data-Fit Parameters

concn, wt %	Q range	PN	L, Å	R, Å	N_{D_2O}
0.25	0.0266–0.15	234	99.2	26.9	10
0.50	0.0266–0.15	238	97.4	27.4	10
1.00	0.0266–0.15	226	98.1	26.6	10
10.0	0.0934–0.264	115	99.0	21.3	19
12.0	0.0934–0.264	106	99.0	21.1	21
15.0	0.0934–0.264	92	99.0	20.5	25
20.0	0.0934–0.264	86	99.0	20.9	30

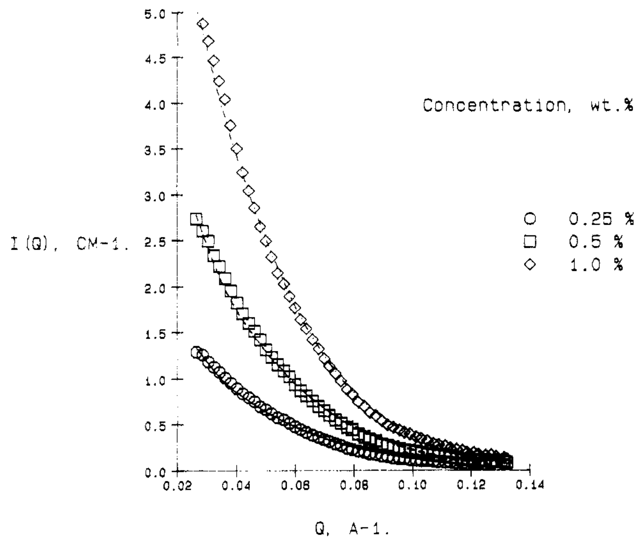

Figure 4. Results of fitting SANS data for solutions in the dilute regime to the cylindrical cross-section formula of eq 2.

ters of the fits are given in Table I. The length of the cylinder is calculated to be 99 Å and the radius of the cylinder 27 Å and the hydration number 10 per repeating unit. Combining this number with eq 4 gives PN = 233. As shown in Figure 1, the transverse dimension of the backbone of one repeating unit l_b = 5.06 Å and the degree of polymerization P is thus determined to be $P = L/5.06 = 19.4$. This number corresponds to the weight-average molecular weight of 7100 which is in excellent agreement with the GPC determination of 6660. The aggregation number per micelle N is equal to $PN/P = 12$. The radius of the cylinder R is approximately equal to the tail length 21.74 Å plus the head group length of 5 Å.

For the high concentration series we fixed the cylinder length at the same value of 99 Å and fitted the data with two adjustable parameters R and N_{D_2O}. The choice of constraint was reasonable, since according to our model depicted in Figure 2, the length of the cylinder is determined by the degree of polymerization P which is determined by synthesis. The only polydispersity allowed by this model is to increase the cylinder length by an integer number for the end to end stacking of the cylinders. This alternative was tried in our analysis but without success.

The Q range for the high concentration series was chosen to be 0.096–0.267 Å^{-1} at which the structure factor $\tilde{S}(Q)$ is assumed to be unity. The choice of the lower limit of Q at 0.096 Å^{-1} is reasonable because it is twice the interaction peak position at Q_{max} = 0.05 Å^{-1}. The results of the fit are displayed in Figure 5 and the fitted parameters given in Table I. The disagreement between the experimental and calculated curves for $Q > 0.17$ Å^{-1} is due to the molecular weight polydispersity of the copolymer, which smears out the oscillatory behavior at larger Q. At this moment, we do not have a model to account for the polydispersity of copolymer micelles. However, we believe that the inclusion of polydispersity may slightly improve the fits but will not change the conclusions on the aggregation numbers.

Three striking trends are noted: (1) the transverse radius R is now reduced to about 21.0 Å which is about the hydrocarbon tail l_t (Figure 1), (2) the hydration number increases from 19 to 30, and (3) the aggregation number N is reduced to 5 or 6, about half of that of the dilute case. We believe our new number of 21.0 Å for the hydrocarbon tail in the concentrated regime is more accurate compared to our previous calculations[10] where the linear approximation was used in the asymptotic analysis. In Figure 6, we display the normalized form factor $\tilde{P}(Q)$ obtained from the fit and the angular-averaged structure factor $\tilde{S}(Q)$ obtained by dividing the measured intensity by $I_0\tilde{P}(Q)$. Notice that the first peak of $\tilde{S}(Q)$ occurs at Q_{max} = 0.05 Å^{-1} with the height of peak at about 1.9. Figure 6 also shows that $\tilde{S}(Q)$ is essentially unity for $Q > 0.09$ Å^{-1}. Figure 7 is the plot of PN (total number of repeating units per micelle) as a function of concentration.

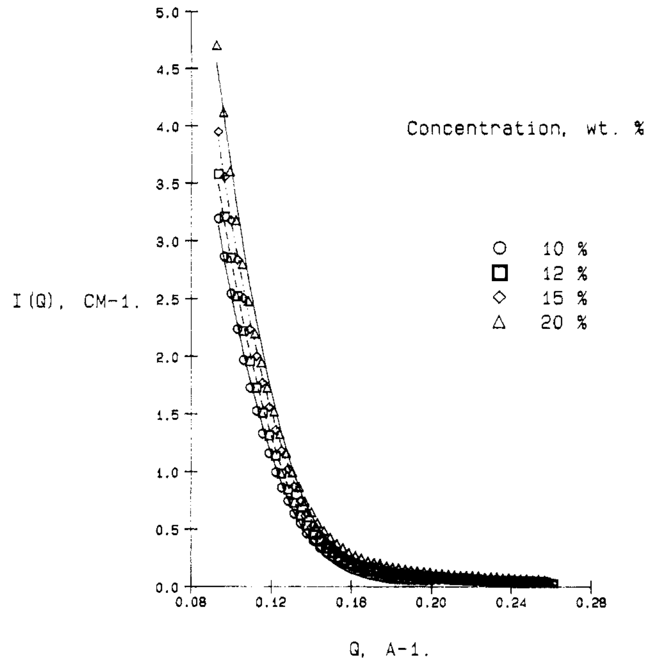

Figure 5. Asymptotic fit of SANS data for solutions in the concentrated regime to the cylindrical-cross section formula of eq 2.

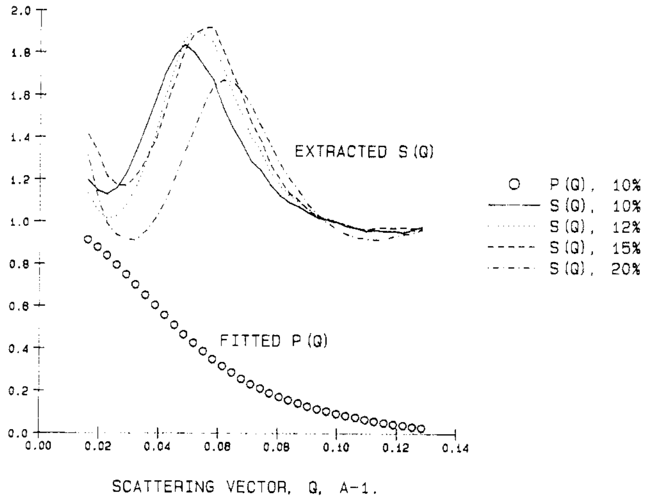

Figure 6. $\tilde{P}(Q)$ and the extracted $\tilde{S}(Q)$ for the high concentration data.

V. Summary and Discussion

We have analyzed SANS data of a charged copolymer in solutions without invoking the detailed calculation of the intermicellar interactions. This is possible by judicious choice of Q range where $\tilde{S}(Q)$ can be safely taken as unity. We have unambiguously established the formation of micelles of this copolymer in solution. In the dilute concentration regime, the aggregation number is 12, however, this number drops precipitously to half of that value, 6–5, in the concentrated regime. The physical reason for this is unknown at the present time but we speculate that it might be due to the fact that for a highly charged polye-

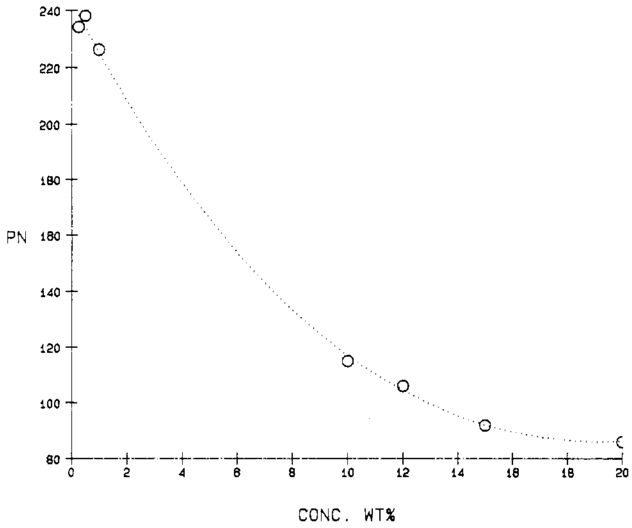

Figure 7. Plot of the number of repeating units per micelle versus concentration.

lectrolyte system like this, the micelles tend to reduce their surface charge densities at high concentrations by reducing their aggregation number to minimize the double-layer repulsive energies and at the same time increase the entropy of dispersion. The reason for a reduced *R* observed at high concentration is related to the penetration of water molecules deeper into the head-group region. The increase of hydration number from 10 at low concentration to 30 at the highest concentration implies that the contrast between the head group and the solvent is gradually lost in this process. The cylinder radius thus appears to be smaller to neutrons. The intermicellar structure factor extracted from the data by dividing it by the micellar form factor (Figure 6) shows an interacting peak occurring at $Q_{\max} = 0.05$ Å^{-1} which moves to larger Q as the concentration increases. Another unusual feature is a rising component above unit at the very small *Q* region. This observation is consistent with SANS data for star-branched polystyrene in a good solvent.[15] In the latter case, when $c > c^*$, an increase in $I(Q)$ is observed at small *Q* and at the same time the maximum at intermediate *Q* is shifted to higher *Q* as the concentration increases. This feature cannot be easily explained without a detailed knowledge of the structure factor of cylindrical micelles, for which some theoretical progress has been made in recent years,[16,17] but a practical method for data analysis has not been proposed.

Acknowledgment. We thank Chuan-Fu Wu of MIT for his assistance in some of the calculations, Dr. Calvin Verbrugge of SCJ for providing the copolymer samples, and Mary Luccas of SCJ for preparing some of the solutions. This work is supported in part by the Intrapreneur Seed Fund from S. C. Johnson & Son, Inc., and an NSF grant to S.H.C.

Registry No. Neutron, 12586-31-1; (maleic anhydride)(1-octadecene) (alternating copolymer, lithium salt), 113109-85-6.

References and Notes

(1) Robb, I. D. In *Surfactant Science Series*: Lucassen-Reynders, E. H., Ed.; Marcel Dekker: New York, 1981; Vol. II.
(2) Dubin, P. L.; Strauss, U. P. In *Polyelectrolytes and Their Applications*; Rembaum, A., Selegny, E., Eds.; D. Reidel: Dordrecht, Holland, 1975; pp 3-13.
(3) Strauss, U. P. In *Microdomains in Polymer Solutions*; Dubin, P. L., Ed.; Plenum: New York, 1985; pp 1-12.
(4) Dubin, P. L.; Strauss, U. P. *J. Phys. Chem.* **1970**, *74*, 2842.
(5) Strauss, U. P. In *Micellization, Solubilization and Microemulsions*; Mittal, K. L., Ed.; Plenum: New York, 1977; Vol. 2.
(6) Shih, L. B.; Luccas, M. H.; Warner, R. J. *Polymer Prepr. (Am. Chem. Soc., Div. Polym. Chem.)* **1986**, *27* (2), 288.
(7) Allaway, J. R., unpublished results.
(8) Okabayashi, H.; Yoshida, T.; Matsushita, K.; Terada, Y. *Chem. Scr.* **1982**, *20*, 117.
(9) Okabayashi, H.; Matsushita, K. In *Surfactants in Solutions*; Mittal, K. L., Lindman, B., Eds.; Plenum: New York, 1984; Vol. 1.
(10) Shih, L. B.; Luccas, M. H.; Chen, S. H.; Lin T. L. *Mater. Res. Soc. Conf. Proc.* **1987**, *79*, 429.
(11) Verbrugge, C. J. U.S. Patent 4 358 573 (example 1).
(12) Warner, R. J.; Krueger, D. A., private communication.
(13) Lin, T. L.; Chen, S. H.; Gabriel, N. E.; Roberts, M. F. *J. Phys. Chem.* **1987**, *91*, 406.
(14) Chen, S. H. *Annu. Rev. Phys. Chem.* **1986**, *37*, 351-99.
(15) Huber, K.; Bantle, S.; Burchard, W.; Fetters, L. J. *Macromolecules* **1986**, *19*, 1404.
(16) Schneider, J.; Hess, W.; Klein, R. *Macromolecules* **1986**, *19*, 1729.
(17) Dhont, J. K. G.; Klein, R. *Colloid Polym. Sci.* **1987**, *265*, 289.

Lattice Models for Bulk Polymers at Interfaces

Doros N. Theodorou

Department of Chemical Engineering, University of California, Berkeley, California 94720, and Center for Advanced Materials, Lawrence Berkeley Laboratory, Berkeley, California 94720. *Received May 27, 1987; Revised Manuscript Received October 23, 1987*

ABSTRACT: Lattice models for the prediction of conformational characteristics and thermodynamic properties at bulk polymer/solid and bulk polymer/gas interfaces are critically examined. Existing models are shown to fall into two broad categories: bond models, in which the probability of a chain conformation is expressed as a product of bond transition probabilities, and site models, in which the probability of a conformation is proportional to a product of probabilities characteristic of the sites occupied by successive chain segments. A general mathematical formulation is developed for bond models, which includes Dill and Flory's model of liquid bilayer membranes and Helfand's model of a pure homopolymer at an interface as special cases. The key assumptions, leading to closure of the bond model equations in each of these two cases, are elucidated.

Introduction

In this series of papers we discuss some lattice approaches for modeling the microscopic structure and thermodynamic properties of bulk polymers at interfaces. We are mainly concerned with polymer/solid, polymer/gas, and polymer/vacuum interfaces, across which there is a relatively abrupt change in polymer segment density. Immiscible polymer/polymer interfaces, for which several theoretical approaches have been developed,[1] will thus not be an object of our investigation. Our interest will focus